World Academy of Science, Engineering and Technology
International Journal of Electronics and Communication Engineering
Vol:8, No:3, 2014

Target and Equalizer Design for Perpendicular Heat-Assisted Magnetic Recording

P. Tueku, P. Supnithi, R. Wongsathan

***Abstract*—**Heat-Assisted Magnetic Recording (HAMR) is one of the leading technologies identified to enable areal density beyond 1 Tb/in^2 of magnetic recording systems. A key challenge to HAMR designing is accuracy of positioning, timing of the firing laser, power of the laser, thermo-magnetic head, head-disk interface and cooling system. We study the effect of HAMR parameters on transition center and transition width. The HAMR is model using Thermal Williams-Comstock (TWC) and microtrack model. The target and equalizer are designed by the minimum mean square error (MMSE). The result shows that the unit energy constraint outperforms other constraints.

***Keywords*—**Heat-Assisted Magnetic Recording, Thermal Williams-Comstock equation, Microtrack model, Equalizer.

I. Introduction

THE proliferation of digital content creation and consumption brings an increasing demand for data storage devices, such as the hard disk drive (HDD). This demand drives requires increasing storage capacity, which in turns drives increasing growth in areal density (AD). AD is defined as the number of bits stored in a bit area of medium and it is determined by the average size of the grains and the number of grains that is used to store 1 bit of information. To increase the AD, the magnetic grain size must be reduced and to maintain the right levels of signal to noise ratio (SNR), the number of grains per bit must be constant. However, small grains will face thermal instability problem. To remedy this issue, media need to have high coercivity (H_c) which means anisotropy (K_u) is high and, therefore, it is difficult to write data bits because the current write field limitation. Heat-assisted magnetic recording (HAMR) channel model has been developed and the thermal Williams-Comstock (TWC) model has been used to predict the limitation. HAMR is one of the four enabling technologies which surpass the critical point of storage density limit known as the super-paramagnetic limit at 1 Tb/in^2 AD, as in [1]-[3].

New write mechanism has been researched by many researchers around the world. It is able to utilize higher anisotropy to produce smaller grain sizes and to secure a signal to noise ratio (SNR) and bit error rate (BER). HAMR can overcome the write field limitation (2.45T) by temporarily reducing H_c during the write process by heating the medium. That means K_u is also reduced and the energy barrier to write on the medium is also decreased. The medium is then rapidly cooled down to the room temperature after magnetization completed, where thermal stability is acceptable.

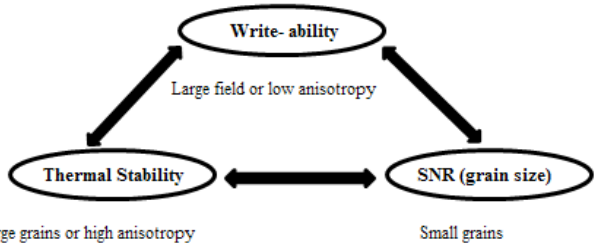

Fig. 1 The write-ability trilemma: the available from writer has to be trade off against thermal stability (large grains or high anisotropy) and media SNR (small grains) [1]

HAMR system has many thermal issues compared to the conventional magnetic recording. Hence, each work step and the whole system need to be researched and clarified, as well as improving the stability and reliability of the system against thermal issues. The HAMR channel model has recently been investigated and the read process of the conventional read channel models employed in current magnetic recording systems has been used to produce the HAMR playback signals, as in [4]-[11].

The organization of this paper is as follows. In Section II, we will describe the principles of perpendicular HAMR systems using the Thermal Williams-Comstock (TWC) model, transition parameters and the microtrack modeling to determine the transition characteristics of both large and non-large spot laser. Next in Section III, we will propose the target and equalizer by the minimum-mean squared error (MMSE) method. Then, the simulation and results is discussed in Section IV. Finally, the conclusion will be made in Section V.

II. Perpendicular Heat-Assisted Magnetic Recording

References [4], [5] show the longitudinal HAMR with large spot approximation is used to simplify the equation but it is only valid if the assumptions are fulfilled. Large spot approximation is also used for the perpendicular HAMR, as in [6]. References [7], [9] show the perpendicular channels with non-large spot approximation are used to simulate the channel model. A linear relationship for remanent magnetization M_r and coercivity H_c with temperature is assumed to be used in [4]-[7] and [9] but as in [10], the non-linear relationship for M_r

P. Tueku is with the International College, King Mongkut's Institute of Technology Ladkrabang, Bangkok 10520 Thailand (phone: 663-527-7345; fax: 663-527-7955; e-mail: S2600622@kmitl.ac.th).

P. Supnithi is with the School of Telecommunications Engineering, King Mongkut's Institute of Technology Ladkrabang, Bangkok 10520 Thailand (e-mail: ksupornc@kmitl.ac.th).

R. Wongsathan is with the Faculty of Engineering, King Mongkut's Institute of Technology Ladkrabang, Bangkok 10520 Thailand (e-mail: s4610146@kmitl.ac.th)

and H_c with temperature T is assumed instead. In this paper, we use the TWC equation for perpendicular HAMR with non-large spot approximation by using linear relationship for M_r and H_c with T to investigate and understand the HAMR system performance.

A. Williams-Comstock (WC) Model

In 1971, Mason Williams and Larry Comstock developed the William-Comstock (WC) model to predict the transition width in longitudinal magnetic recording, as in [13]. They provide a simple analysis of the write process. WC model is a well-known approximate analytical model which describes the transition characteristics in a conventional magnetic recording system. In the model, the "zigzag" nature of magnetic transition is ignored and the shape of magnetic transition is presumed to be described by the arctangent function. The transition center x_0 and the transition parameter a are the two main parameters which can be derived from this model.

The relationship between the applied field H_a and the resultant magnetization M in the medium is given by the hysteresis loop of the medium and can be written as $M=F_{\text{loop}}(H_a)$, where F_{loop} represents the hysteresis loop. The applied magnetic field during the transition formation can be described by the contribution from the head field H_h and the demagnetization field H_d from the recorded transition, i.e.,

$$H_a(x) = H_h(x) + H_d(x) \tag{1}$$

In the down track direction (x-direction), M can be determined by solving

$$M(x) = M\left[H_a(x)\right] = M\left[H_h(x) + H_d(x)\right] \tag{2}$$

where H_d is dependent on M in (2), and so (2) can only be solved by iteration. Williams and Comstock noted that is possible to solve the derivative of (2) by evaluating at the transition center x_0 where the applied field at x_0 is equal to the coercivity H_c. The WC slope equation can be derived from (2)

$$\left.\frac{dM(x)}{dx}\right|_{x_0} = \left.\frac{dM(H)}{dH_a}\right|_{H_c} \left.\frac{dH_a(x)}{dx}\right|_{x_0} = \left.\frac{dM(H)}{dH_a}\right|_{H_c} \left[\left.\frac{dH_h(x)}{dx}\right|_{x_0} + \left.\frac{dH_d(x)}{dx}\right|_{x_0}\right] \tag{3}$$

The magnetization transition during recording can be described by the arctangent function, both the magnetization gradient *dM/dx* and demagnetization field gradient *dHd/dx* can be expressed analytically in terms of only one unknown quantity, namely, the transition parameter a. Furthermore, the head field gradient *dHh/dx* and magnetization gradient with applied field *dM(H)/dHa* can be evaluated from the analytic Karlqvist head field expressions and the M–H loop for the medium. These assumptions allow (3) to be solved analytically, giving an expression for a containing all the relevant factors in the write process.

B. Thermal Williams-Comstock (TWC) Model

$F_{loop}(H_a)$ in WC model does not account for the effects of heating in HAMR system. In 2004, WC model was extended by incorporating thermal gradients of coercivity H_c and magnetization M for a longitudinal HAMR system and is known as the Thermal Williams–Comstock (TWC) model, as in [4]. The effective field (h) is introduced to account for heating behavior, i.e.,

$$h(x) = \frac{H_a(x)}{H_c(T(x))}. \tag{4}$$

The dependence of M on the temperature captured by h in (4) is substituted into $M=F_{loop}(h)$. Evaluating the derivative of $M(x)$ at x_0, where the applied field is equal to coercivity $H_a=H_c$, we obtain

$$\left.\frac{dM(x)}{dx}\right|_{x_0} = \left.\frac{dM(h)}{dh}\right|_{H_c} \left.\frac{dh(x)}{dx}\right|_{x_0} \tag{5}$$

The derivative at the H_c is simply the linear slope and S^* is coercivity squareness factor.

$$\left.\frac{dM(x)}{dx}\right|_{H_c(T(x_0))} = \frac{M_r(T(x_0))}{(1-S^*(T(x_0)))} = \left.\frac{H_c(T(x_0))dM(H)}{dH_a}\right|_{H_c(T(x_0))} \tag{6}$$

The thermal Williams-Comstock slope equation can then be derived from (3) giving

$$\left.\frac{dM(x)}{dx}\right|_{x_0} = \left.\frac{dM(H)}{dH_a(T(x_0))}\right|_{H_c(T(x_0))} \times \left[\left.\frac{dH_h(x)}{dx}\right|_{x_0} + \left.\frac{dH_d(x)}{dx}\right|_{x_0} - \left.\frac{dH_c(T(x_0))}{dT}\right|_{T(x_0)} \left.\frac{dT}{dx}\right|_{x_0}\right]. \tag{7}$$

Since dM/dx and dH_d/dx depend on a, a can be solved by using (4). To obtain dM/dx, it is assumed that the transition during recording can be described by the arctangent function from which dM/dx can be derived.

$$M(x) = \frac{2M_r(T(x))}{\pi} \tan^{-1}\frac{x-x_0}{a} \tag{8}$$

and dM/dx at x_0 can be solved by differentiating (8), i.e.,

$$\left.\frac{dM(x)}{dx}\right|_{x_0} = \frac{2M_r(T(x_0))}{\pi a} \tag{9}$$

The term $dM(h)/dh$ from (5) at x_0 can be solved as slope of hysteresis loop is always positive at either transition is made from positive or negative H_c

$$\left.\frac{dM(h)}{dh}\right|_{H_c(T(x_0))} = \left|\frac{1}{H_c(T(x_0))} \times \frac{M_r(T(x_0))}{1-S^*}\right| \quad (10)$$

The term dH_h/dx of perpendicular recording at x_0 can be solved by using and the symmetry of the longitudinal Karlqvist head field component. The perpendicular head field can be derived by facilitating to turned sideways of longitudinal as

$$H_h = \frac{H_0}{\pi}\left[\tan^{-1}\left(\frac{y+g/2}{x}\right) - \tan^{-1}\left(\frac{y-g/2}{x}\right)\right], \quad (11)$$

and

$$\left.\frac{H_h(x)}{dx}\right|_{x_0} = -\frac{gH_0}{\pi\left(x^2+(g/2)^2\right)}, \quad (12)$$

where H_0 is the deep gap field, g is the gap width between pole head and its image ($g = 2d+2t$), t is the medium thickness and the field is evaluated at the center of medium ($y = t/2$). The parameter H_d for perpendicular recording is obtained by convolving the unit step response at the original and the magnetization gradient, i.e.,

$$H_{d,perp} = -\frac{\partial M(x)}{\partial x} * H_y^{step} = -\frac{\partial M(x)}{\partial x} * \frac{1}{\pi}\tan^{-1}\left(\frac{2x}{t}\right) \quad (13)$$

$$\frac{dH_d(x)}{dx} = -\frac{4}{\pi^2}\int_{-\infty}^{\infty}\frac{M_r(T(x'))a}{a^2+(x'-x_0)^2}\frac{t}{t^2+4(x-x')^2}dx' + \frac{4}{\pi^2}\int_{-\infty}^{\infty}\tan^{-1}\left(\frac{x'-x_0}{a}\right)\left.\frac{dM_r(T(x'))}{dT}\right|_{T(x')}\frac{dT(x')}{dx'}\frac{t}{t^2+4(x-x')^2} \quad (14)$$

Here, H_c and M_r are linearly temperature-dependent (T), i.e.

$$H_c = -H_{c0}T(x,y) + H_{c,const} \quad (15)$$

$$M_r = -M_{r0}T(x,y) + M_{r,const} \quad (16)$$

where H_{c0} and M_{r0} are the temperature sensitivities of H_c and M_r, $H_{c,const}$ and $M_{r,const}$ are H_c and M_r at 0 Kelvin (K). So dH_c/dT is $-H_{c0}$ and dM_r/dT is $-M_{r0}$. A two-dimensional (2D) Gaussian thermal profile is given as

$$T(x,z) = T_{peak}\exp\left(-\frac{(x-c_0)^2}{2\sigma_t^2}\right)\exp\left(-\frac{z^2}{2\sigma_t^2}\right) + 300 \quad \text{(K)} \quad (17)$$

where T_{peak} is the peak temperature in the medium above room temperature in degree Celsius, c_0 is the laser spot position, x is defined to the position in down-track direction and z is defined to the position in cross-track direction. Differentiating (17), we have

$$\frac{T(x,z)}{dx} = T_{peak}\left(-\frac{(x-c_0)}{\sigma_t^2}\right)\exp\left(-\frac{(x-c_0)^2}{2\sigma_t^2}\right)\exp\left(-\frac{z^2}{2\sigma_t^2}\right) \quad (18)$$

C. Transition Center (x_0) and Transition Parameter (a)

The position x_0 is defined as the point where the medium reverses its direction of magnetization and a is measured and related to the width of the magnetization transition. Achieving the narrowest possible transition (smallest a) allows placing recording bits close together and hence results in high linear density. The position x_0 of perpendicular HAMR with large spot and linear relationship for H_c and M_r can be calculated, as in [9],

$$x_0 = \frac{g+\sqrt{g^2 - a\tan^2\left(\pi\frac{H_c(T(x_0))}{H_0}\right)\left(y^2-(g/2)^2\right)}}{2\tan\left(\pi\left(\frac{H_c(T(x_0))}{H_0}\right)\right)} \quad (19)$$

and a can be also calculated from

$$a = -\frac{\gamma}{2} + \frac{1}{2}\sqrt{\gamma^2 + \frac{4H_c(1-S^*)t}{\Delta\pi}}\Bigg|_{x_0} \quad (20)$$

where

$$\Delta \equiv \frac{H_g g}{\pi\left(x_0^2+(g/2)^2\right)} - \frac{dH_c}{dT}\left.\frac{dT}{dx}\right|_{x_0}$$

and

$$\gamma \equiv \frac{2M_r}{\Delta\pi} - \frac{t}{2} + \frac{2H_c(1-S^*)}{\Delta\pi}$$

For non-large spot HAMR, x_0 can be solved by

$$x0,\ j+1 = \frac{g+\sqrt{g^2 - 4\tan^2\left(\pi\frac{H_c(T(x_0))+H_d(x_0,j,a_k)}{H_0}\right)\left(y^2-(g/2)^2\right)}}{2\tan^2\left(\pi\frac{H_c(T(x_0))+H_d(x_0,j,a_k)}{H_0}\right)} \quad (21)$$

and a can be solved by

$$a_{k+1} = \frac{-\beta+\sqrt{\beta^2+4\pi(\alpha+\delta)H_c(1-S^*)t}}{2\pi(\alpha+\delta)} \quad (22)$$

where

$$\alpha = \frac{H_g g}{\pi\left(x_{0,j+1}^2+(g/2)^2\right)}, \delta = \frac{dH_d\left(a_k, x_{0,j+1}\right)}{dx} - \frac{dHc}{dx},$$

$$\beta = -\frac{\pi\alpha t}{2} + 2M_r - \frac{\pi t}{2}\left(\frac{dH_d\left(a_k, x_{0,j+1}\right)}{dx} - \frac{dH_c}{dx}\right) + 2H_c(1-S^*)$$

D.Microtrack Model

The microtrack model is used for 2D process of heating and magnetization of a medium to solve the problem of determining the transition characteristics in HAMR by dividing recorded track into N individual sub-tracks of equal width with different transition parameters. The TWC equation is applied to determined x_0 and a in each individual sub-track, as in [4]-[9]. The playback voltage (V) of perpendicular recording is given from [12] by

$$V(x,a_i,x_{0,i}) = -CM_r t \ln\left(\frac{\left(g_r/2-(x-x_{0,i})\right)^2+\left(d+a_i+t/2\right)^2}{\left(g_r/2+(x-x_{0,i})\right)^2+\left(d+a_i+t/2\right)^2}\right) \quad (23)$$

where C is a system specific constant, g_r is the read head gap, and d is the head-medium spacing and t is denote to media thickness.

The overall transition response $p(x)$ can be obtained by weighting the transition response $p_i(x)$ of each sub-track to obtain

$$p_i(x) = \exp\left(\frac{\left(-\frac{N+1}{2}\Delta z+i\Delta z\right)^2}{2\sigma_r^2}\right)\cdot V(x,a_i,x_{0i}) \quad (24)$$

and

$$p(x) = \frac{1}{N}\sum_{i=1}^{N} p_i(x) \quad (25)$$

where a_i and x_{0i} are the transition parameter and transition center of the i^{th} microtrack, i can be 1 to N and Δz stands for the width of each sub-track. The bit response is then

$$h(x) = 0.5\{p(x)-p(x-T_x)\} \quad (26)$$

where T_x denotes the along-track bit period.

III. Target and Equalizer Design

A. Channel Model

The laser can be positioned either in the direction of the head movement (up-track or $+x$) or opposite to it (down-track or $-x$). However, in this work, the laser is assumed to be at the center of the track in the cross-track direction. The HAMR channel with equalizer design is shown in Fig. 2.

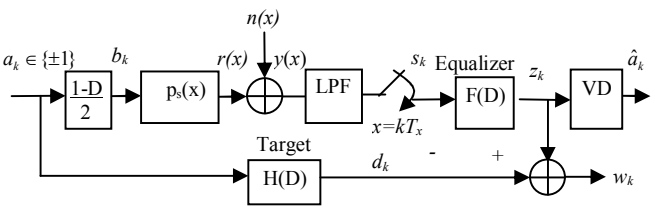

Fig. 2 The HAMR system with target-shaping equalization

where $a_k \in \{\pm 1\}$ is input sequences and filtered by using ideal differentiator (1-D)/2. The sequence of the transitions is $b_k \in \{\pm 1, 0\}$, where $b_k \in \{\pm 1\}$ represents the positive and negative transitions, and b_k = 0 means no transition. The playback signal $r(x)$ is obtained by convolution between b_k and transition response p_k and then corrupted by the additive white Gaussian noise (AWGN). In this simulation, SNR is defined as SNR = $10\log_{10}(1/\sigma^2)$, where σ^2 is the variance of AWGN. The playback signal with AWGN $y(x)$ will be passed to low pass filter (LPF), sampled and then put in equalizer (FD) to equalize the signal in order to facilitate the application of Viterbi detector (VD). Finally, the equalized outputs $z(k)$ are detected by VD.

B. Target and Equalizer Design

In this study, we design targets (HD) and equalizers (FD) by using the minimum-mean squared error (MMSE) method to minimize the mean-squared error (MSE) between desired outputs and equalizer outputs, as in [11], [14]. The target $H(D)$ and its corresponding $F(D)$ can be obtained by minimizing

$$E\left\{w_k^2\right\} = E\left[\left(z_k-d_k\right)^2\right] = E\left[\left\{(s_k*f_k)-(a_k*h_k)\right\}^2\right] \quad (27)$$

where w_k is the difference between output of equalizer, z_k and the desired output, d_k of designed target, * is the convolution operator and $E\{.\}$ is the expectation operator, h_k and f_k stand for the coefficients of $H(D)$ and $F(D)$. The MMSE can be expressed as

$$\varepsilon^2 = E\left\{w_k^2\right\} = \mathbf{F}^T\mathbf{R}\mathbf{F} + \mathbf{H}^T\mathbf{A}\mathbf{H} - 2\mathbf{F}^T\mathbf{P}\mathbf{H} \quad (28)$$

where $\mathbf{H} = [h_0\ h_1\ h_2\ \ldots\ h_{L-1}]^T$ represents the L–tap GPR target and $\mathbf{F}=[f_{-K}, f_{-K+1}, \ldots f_0\ \ldots\ f_K]^T$ represents the K-tap equalizer by where the length of the equalizer is N ($N = 2K+1$). $\mathbf{A}$ is an LxL autocorrelation matrix of a_k, R is an MxM autocorrelation matrix of sequence s_k, and $\mathbf{P}$ is an MxL cross-correlation matrix sequence of a_k and s_k. During the minimization process, the specified constraint must be used to avoid the trivial solution of $\mathbf{F} = \mathbf{0}$ and $\mathbf{H} = \mathbf{0}$.

Firstly, by minimizing (28) subject to a monic constraint, we fix h_0=1 and compute

$$\begin{aligned}
&\varepsilon^2 = \mathbf{F}^T\mathbf{R}\mathbf{F} + \mathbf{H}^T\mathbf{A}\mathbf{H} - 2\mathbf{F}^T\mathbf{P}\mathbf{H} - 2\lambda\left(\mathbf{I}^T\mathbf{H}-1\right)\\
&\lambda = \frac{1}{\mathbf{I}^T\left(\mathbf{A}-\mathbf{P}^T\mathbf{R}^{-1}\mathbf{P}\right)^{-1}\mathbf{I}}\\
&\mathbf{H} = \lambda\left(\mathbf{A}-\mathbf{P}^T\mathbf{R}^{-1}\mathbf{P}\right)^{-1}\mathbf{I}\\
&\mathbf{F} = \mathbf{R}^{-1}\mathbf{P}\mathbf{H}
\end{aligned} \quad (29)$$

where λ is the Lagrange multiplier and $\mathbf{I}$ is an L-element column vector which 1st element is 1 and the rest is 0. Secondly, we fix the second target h_1=1 constraint. Column vector $\mathbf{J}$ that 2nd element is 1 and the others are 0. This is identical to monic constraint solution but $\mathbf{I}$ is replaced by $\mathbf{J}$. Thirdly, the energy $\mathbf{H}^T\mathbf{H}$=1 is fixed to minimize (28) called the unit energy constraint.

$$\varepsilon^2 = \mathbf{F}^T\mathbf{R}\mathbf{F} + \mathbf{H}^T\mathbf{A}\mathbf{H} - 2\mathbf{F}^T\mathbf{P}\mathbf{H} - 2\lambda\left(\mathbf{H}^T\mathbf{H}-1\right) \quad (30)$$

After differentiating and setting the result to 0, the final constraint we use fixed target constraint according to PR form 1-D^2 of the PR-4 target for minimizing (28).

IV. Simulation Results

In this work, the medium is assumed to be $Fe_{55-x}Ni_xPt_{45}L1_0$ where 10<x<30% because the linear relationship for remanent magnetization M_r and coercivity H_c with temperature is resulted in this range, as in [9], [10]. For all cases, the laser is assumed to be at the center of the track in the cross-track direction but varied in the down-track direction. The temperature induced by the laser is assumed to be Gaussian in both dimensions with the peak temperature of 330°C and track width 20nm. System parameters are given in Table I.

We first discuss the results from Fig. 3. Firstly, we fix M_r magnetization dependencies on temperature to study the behavior of x_0 and a by using various H_c. With magnetization dependencies on temperature (M_r=-1000T+1.8x10^6), we found that at increasing H_c, x_0 is shifted faraway from laser position and a is decreased. Secondly, we vary M_r to study x_0 and a by using H_c = -2900T+2.4x10^6 for evaluation. Fig. 4 shows that x_0 has almost the same values and small a is found at low M_r. Small a means narrow transitions, hence, recording bits are packed close together.

Next, we study x_0 and a by focusing on the head field (H_0). The results show that x_0 is shifted far from the laser position and a is wider at high head field as shown in Fig. 5. Finally, using high H_c, low M_r and low H_0 to evaluate the system by varying peak temperature (T_{peak}), the results of this experiment show that high T_{peak} will give small a as shown in Fig. 6.

As the discussion before, we select high H_c, low M_r, low H_0 and high T_{peak} to evaluate the system. The transition response $p(x)$ and bit response $h(x)$ can be achieved and shown in Fig. 7. We get PW_{50} equal to 13.988 nm and hence ND is about 2. The HAMR playback signal is obtained by the convolution between b_k and p_x and corrupted from AWGN. The playback with and without AWGN is shown in Fig. 8. Playback signal from LPF is also shown in this Fig. 8.

For MMSE equalizer design, we use the fixed target constraint to minimize the MSE by setting the various number of equalizer taps. Equalizer taps are in the range of 3 to 21 taps. PR1 gives the lowest MMSE from all the targets for this case. The results are shown in Fig. 9. The MMSE value at 11-tap equalizer is equal to 0.526. The 11-tap equalizer coefficients are [0.044 -0.036 0.252 0.128 1.320 2.641 1.356 0.404 0.166 0.033 -0.010]

Next, we compare the MSE using four target constraints for evaluation and the range is from 3 to 21 taps. We use 3-tabs target to simulate this comparison. The result shows that the unit energy constraint has the lowest minimum MSE, as in Fig. 10. The 3-tap target with 11-tap equalizer has the MSE equal to 0.065. The h_1=0 constraint gives the MSE of 0.105. For h_0 = 1 constraint, the minimum MSE of this targets is 0.091, and the fixed-target constraint using PR2 [1 2 1] has the highest MSE value equal to 1.890.

Since the unit-energy constraint gives the lowest MSE value, we select the unit energy constraint to evaluate and find the MSE with the various number of target taps. Equalizer taps are also in the range of 3 to 21 taps as the previous simulation. For the 11-tap equalizer, the 10-tap target gives the minimum MSE as shown in Fig. 11. The 11-tap equalizer coefficients are [-0.043 0.050 -0.126 0.186 -0.466 0.228 0.616 -0.956 0.360 0.413 -0.438] and 10-tap target coefficients are [-0.261 0.475 -0.109 -0.491 0.607 -0.142 -0.212 0.132 -0.039 0.021]. The MMSE value is 0.055.

V. Conclusions

In this paper, we use the thermal William-Comstock equation to model the perpendicular heat assisted magnetic recording with non-large thermal laser spot. The playback signal of HAMR can be affected from various parameters such as H_c. M_r, H_0 and T_{peak}. The simulation results show that the proper high H_c, low M_r, low H_0 and high T_{peak} provide the good transition parameters. Moreover, we design the MMSE equalizer for heat-assisted magnetic recording. The lowest minimum MSE value is obtained from the unit energy constraint.

TABLE I
System Parameters

Symbol	Parameter	Unit
TW	track width	20 nm
N	number of sub-track	10
c_o	laser position	0 nm
H_0	deep gap field	1x10^6 A/m
T_{peak}	peak temperature	330 C°
σ_t	sigma of temperature profile	16.2 nm
g	gap width between pole head and its image	32 nm
σ_r	sigma of reader sensitivity function	4.23 nm
d	head-medium distance or fly height	6 nm
t	medium thickness	10 nm
T_x	bit period	6 nm
C	a system specific constant	1
H_c	dependence of coercivity on temperature	2900T+2.4x 10^6 A/m
M_r	dependence of remanent magnetization on temperature	600T+1.8x1 0^6 A/m
AD	Areal density	5 Tb/in^2

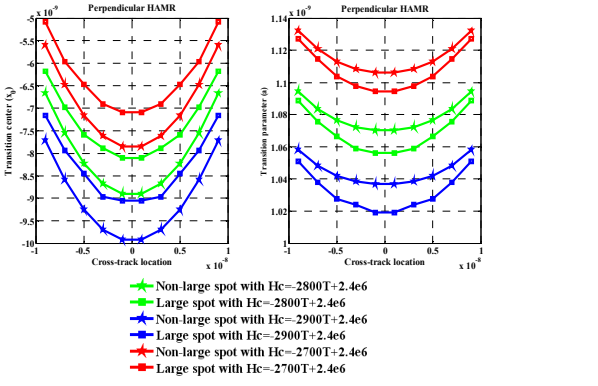

Fig. 3 Transition center and parameter with various H_c dependencies on temperature

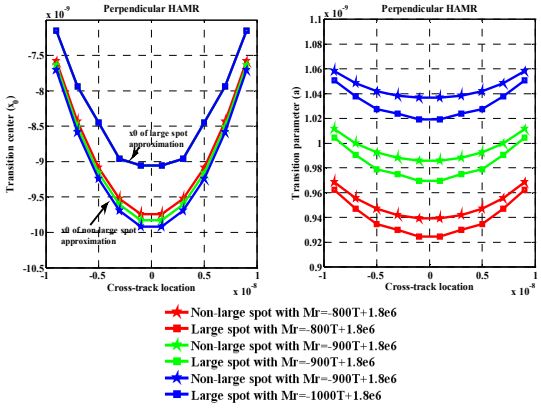

Fig. 4 Transition center and parameter with various M_r dependencies on temperature

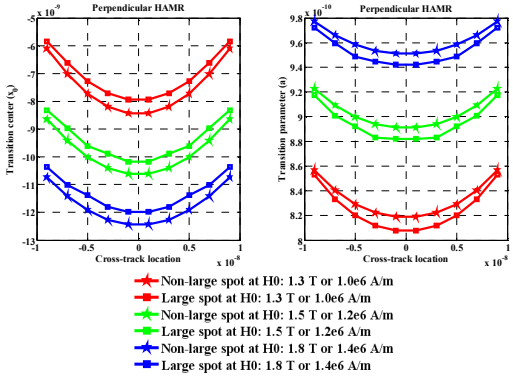

Fig. 5 Transition center and parameter with various head field

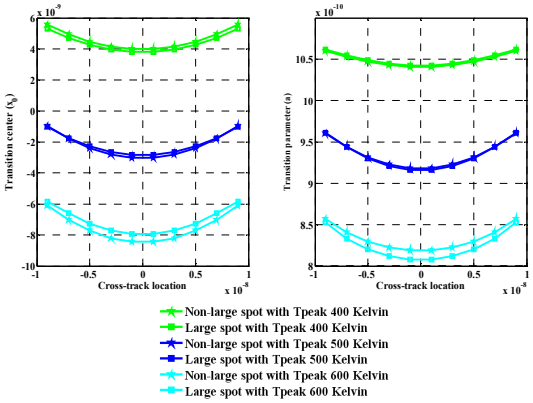

Fig. 6 Transition center and parameter with various peak temperatures

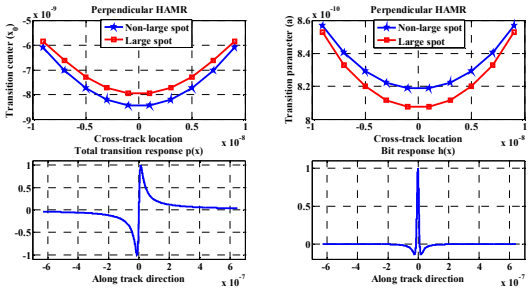

Fig. 7 Transition center, parameter, response and bit response

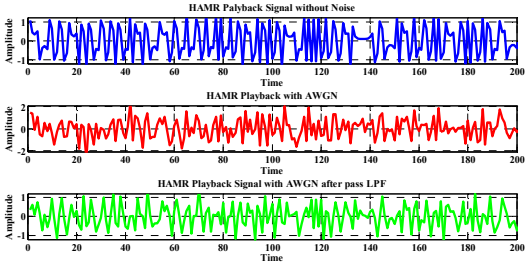

Fig. 8 Playback signal with and without AWGN

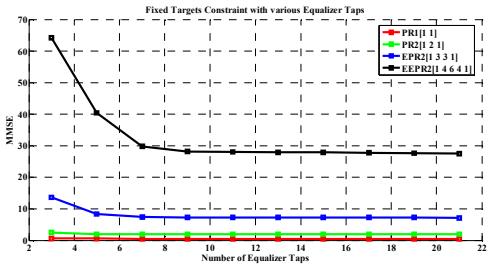

Fig. 9 MMSE of fixed-target constraint with various equalizer taps

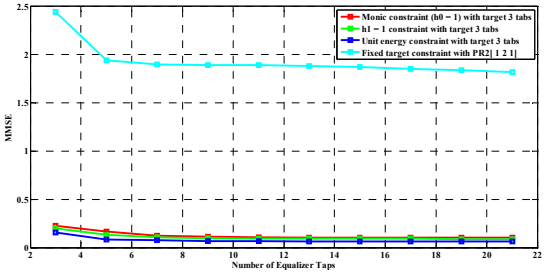

Fig. 10 MMSE of various targets constraint using 3 target taps

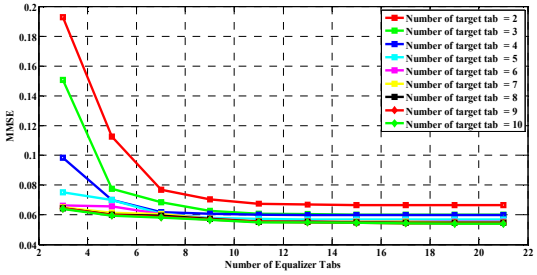

Fig. 11 MMSE of unit-energy constraint equalizers with various target tabs

ACKNOWLEDGMENT

This work was support in part by Faculty of Engineering, King Mongkut's Institute of Technology Ladkrabang. Also, we would like to acknowledge Western Digital (Thailand) Co., Ltd. for granting the scholarship at the International College, King Mongkut's Institute of Technology Ladkrabang.

REFERENCES

[1] O. Heinonen and K.Z Gao, "Extension of perpendicular recording," *Journal of Magnetism and Magnetic Material*, 2008, pp.2885-2888.
[2] Y. Shiroishi, K. Fukuda et al., "Future Options for HDD Storage," *IEEE Trans. Magn.*, vol. 45, no. 10, pp. 3816-3822, Oct. 2009.

[3] E.M. Kurtas, M.F. Erden et al., "Future read channel technologies and challenges for high density data storage applications, Acoustics, Speech, and Signal Processing," Proceedings of *ICASSP* 2005, pp. 737-740.
[4] T. Rausch, J.A. Bain, D.D. Stancil, and T.E. Schelsinger, "Thermal Williams-Comstock model for predicting transition lengths in heat-assisted magnetic recording system," *IEEE Trans. Magn.*, vol. 40, no. 1, pp. 137-147, Jan. 2004.
[5] M.F. Erden, T. Rausch, W.A. Challener, "Cross-track location and transition parameter effects in heat-assisted magnetic recording," *IEEE Trans. Magn.*, vol. 41, no. 6, pp.2189-2194, Jun. 2005.
[6] R. Radhakrishnan, M.F. Erden et al., "Transition Response Characteristics of Heat-Assisted Magnetic Recording and Their Performance With MTR Codes," *IEEE Trans. Magn.*, vol. 43, no. 6, pp. 2298-2300, Jun. 2007.
[7] R. Radhakrishnan, B. Vasic, M.F. Erden et al., "Characterization of of Heat-Assisted Magnetic Recording Channels," *DIMACS Series in Discrete Mathematic sand Theoretical Computer Science*, vol. 73, pp. 25-41, 2007.
[8] M.H. Kryder, E.C. Gage et al., "Heat-Assisted Magnetic Recording," *Invited Paper Proceedings of the IEEE*, vol. 96, no. 11: 1810-1835, Noember. 2008.
[9] R. Wongsathan and P. Supnithi "Channel response of HAMR with linear temperature-dependent coercivity and remanent magnetization," in *Conf. Rec. 2012 IEEE Int Conf. ECTI-CON*, 2012, pp. 1-4.
[10] J.U. Thiele, K.R. Coffey, M.F. Toney, J.A. Hedstrom, and A.J. Kellock, "Temperature dependent magnetic properties of highly chemically ordered $Fe_{55-x}Ni_xPt_{45}L1_0$ films," *J. Appl. Phys.*, vol. 91, no. 10, pp. 6595-6600, May 2002.
[11] P. Kovintavewat, I. Ozgunes, E. Kurtas, J.R. Barry and S.W. McLaughlin, "Generalized Partial-Reaponse Targets for Perpendicular Recording with Jitter Noise," *IEEE Trans. Magn.*, vol.38, no.5, pp. 2340-2342, Sep. 2002.
[12] H.N. Bertram, *Theory of Magnetic Recording*. Cambridge, U.K.: Cambridge Univ. Press 1994, ch. 5, pp. 107-138.
[13] B. Vasic and E.M. Kurtas, *Coding and Signal Processing for Magnetics Recording Systems*, Boca Raton, CRC PRESS 2005, ch. 2, pp. 2.2-1-2.2-26.
[14] P. Kovintavewat, *Signal Processing for Digital Data Storage Volume II: Receiver Design*, National Electronics and computer Techonology Center(NECTEC) 2007, ch. 3, pp. 43-64.